An Optical Super-Microscope for Far-field, Real-time Imaging Beyond the Diffraction Limit

Supplemental Information

Alex M. H. Wong[1], George V. Eleftheriades[1*]

1Rogers S. Sr. Department of Electrical and Computer Engineering, University of Toronto. 10 King's College Rd., Toronto, ON, M5S 3G4, Canada.

Alex M. H. Wong (alex.wong@mail.utoronto.ca),

George V. Eleftheriades (gelefth@waves.utoronto.ca).

1. Effect of Small Circular Apertures

In this work, we used a 10 μm circular aperture to experimentally measure the PSF of our OSM, and performed two-point resolution experiments with 15 μm apertures. Supplementary Figure S7 compares the calculated PSF of an imaging system with λ = 632.8 nm and NA = 0.00864 with an image this system would produce of a circular aperture with 15 μm diameter. The plot is created along the cross-section y = 0. The fact that the two waveforms are near-identical validates our use of these apertures. For the following section we will use 15 μm apertures to calculate an equivalent Rayleigh criterion for coherent imaging systems.

2. Diffraction Limit for a Coherent Imaging System

According to the Rayleigh criterion, the minimum resolvable distance between pinholes is given by

$$R = \frac{0.61\lambda}{NA}. \quad \text{(S1)}$$

At this distance, two incoherent pinholes would be reasonably resolved at the image plane, with the midpoint between the point images attaining an intensity 73% that of the peaks. However, coherent objects image differently, since one must add the image fields, not intensities, of the respective point objects being imaged. Thus, as pointed out in Supplementary ref. 1, the phase variation between point objects greatly influences the minimum resolvable distance in a coherent imaging scheme. For our work, a normally incident laser beam illuminated two small circular apertures in phase. Hence their image fields interfere constructively to preclude their resolution at 0.61λ/NA. Nonetheless, as Supplementary Figure S8 shows, the small apertures would eventually be resolved as the separation distance increases; and at 0.82λ/NA, the intensity dip in the midpoint of the two point images reach the same level as under the Rayleigh criterion in

incoherent imaging. We may regard this as an equivalent Rayleigh criterion for coherent imaging, under the context of normal illumination and small observation angles.

References

1. Goodman, J. *Introduction to Fourier Optics* (Roberts and Company, Englewood, 2004).

Supplementary Figures

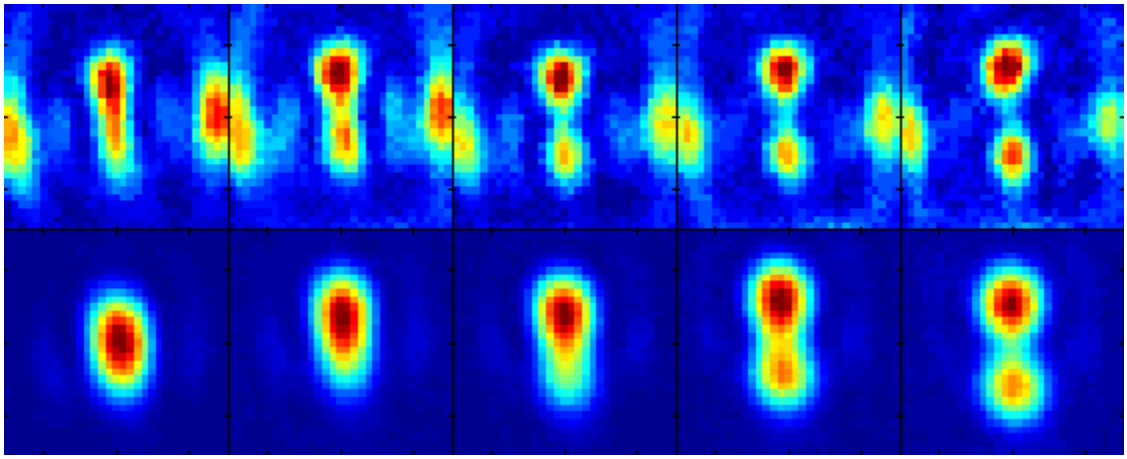

Supplementary Figure S1 | Comparison in resolving closely spaced apertures (III). Close ups of 2-point resolution images, for two 15 μm apertures, separated vertically by distances of 40 μm, 45 μm, 50 μm, 55 μm and 60 μm respectively, from left to right. The top row shows a close up of the superoscillatory image, while the bottom row shows the corresponding view with the diffraction-limited system.

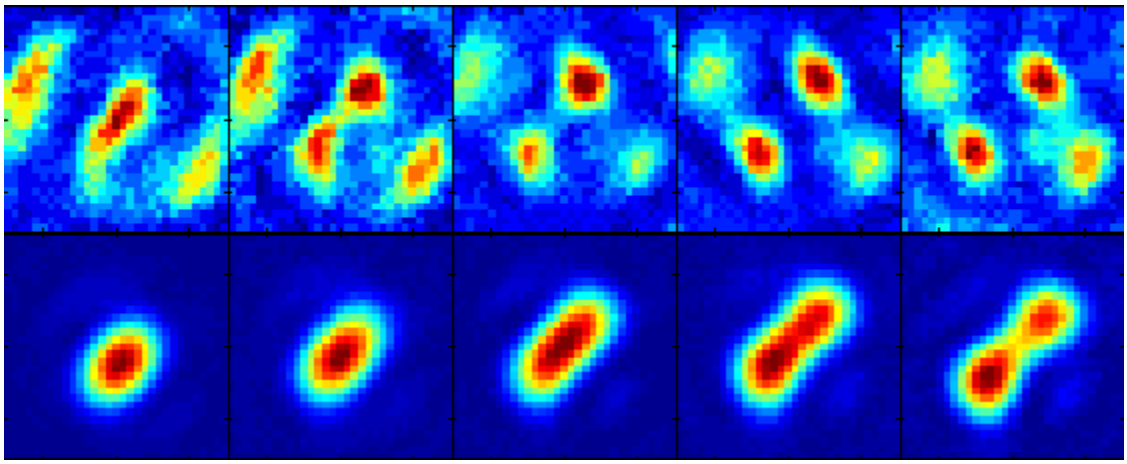

Supplementary Figure S2 | Comparison in resolving closely spaced apertures (IV). Close ups of 2-point resolution images, for two 15 μm apertures, separated diagonally by distances of 35.3 μm, 42.4 μm, 49.5 μm, 56.5 μm and 63.7 μm respectively, from left to right. The top row shows a close up of the superoscillatory image, while the bottom row shows the corresponding view with the diffraction-limited system.

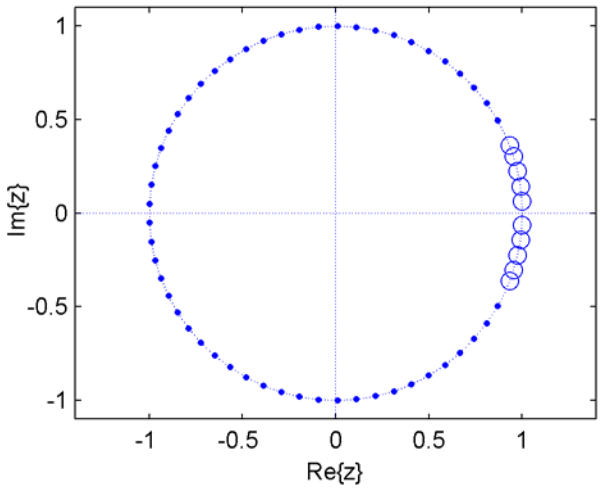

Supplementary Figure S3 | A plot of zeros locations which form the output of the 1D superoscillatory function design algorithm. The principle period of $F(x)$ traces along the unit circle, from angle$[-\pi,\pi]$. Open circles denote zeros in the superoscillatory design region; solid dots denote zeros in the sideband region.

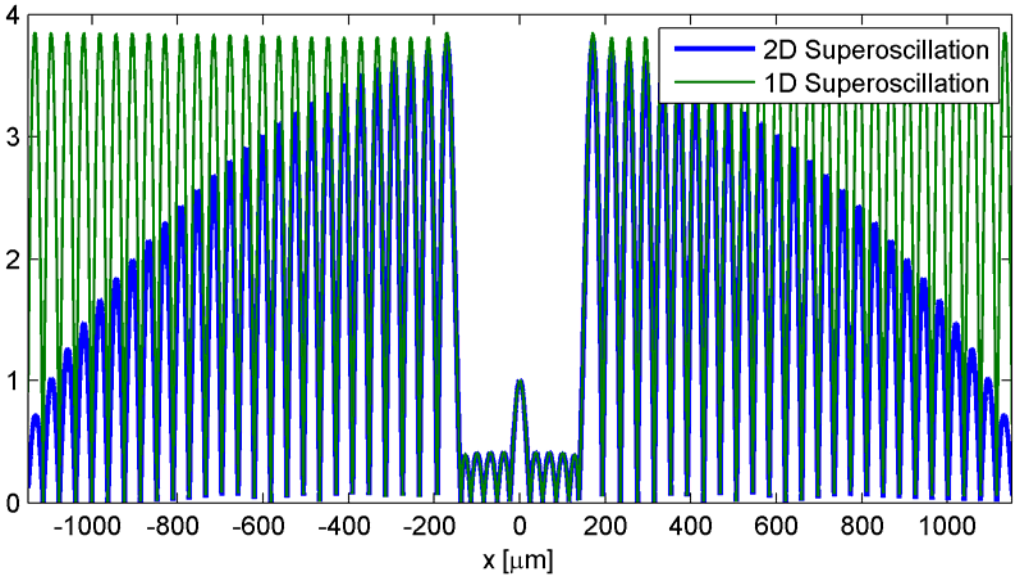

Supplementary Figure S4 | A comparison of 1D and 2D superoscillatory functions, designed such that they share the same null locations. It is evident that the two functions have very similar profiles, especially inside the superoscillatory region.

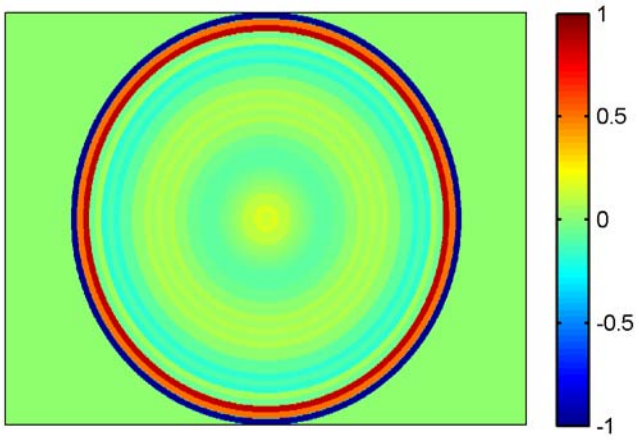

Supplementary Figure S5 | A plot of the designed transmission function. Each ring has width Δk, and transmission weighting proportional to $[b_0,\ldots,b_p]$ from equation (6). This transmission function was spatially mapped onto the SLM superpixel array to implement the optical transfer function of the OSM.

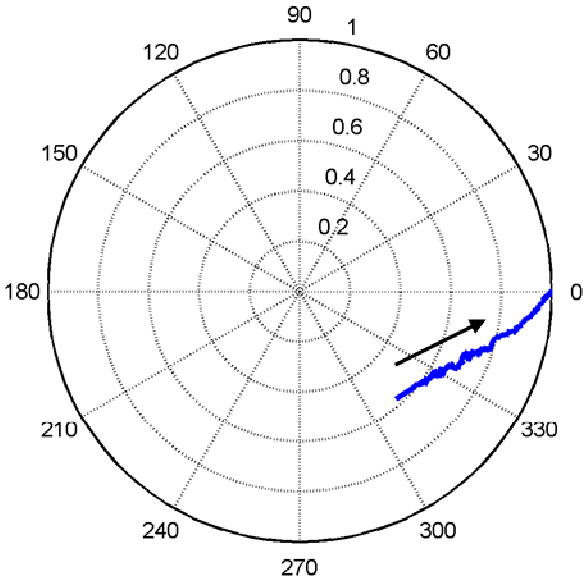

Supplementary Figure S6 | A plot of the spatial light modulator's reflection coefficient, $r(l)$, for $l = 25$ to $l = 255$. All values are normalized to $r(l = 255)$. The arrow points in the direction of increasing l.

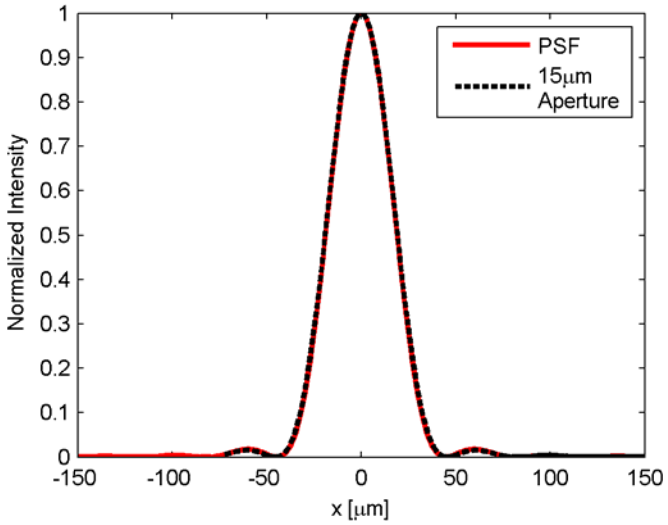

Supplementary Figure S7 | A comparison of the PSF of a diffraction-limited imaging system with a calculated image of a small circular aperture. The diffraction-limited imaging system has λ = 632.8 nm and NA = 0.00864. The comparison shows that the two waveforms are nearly identical.

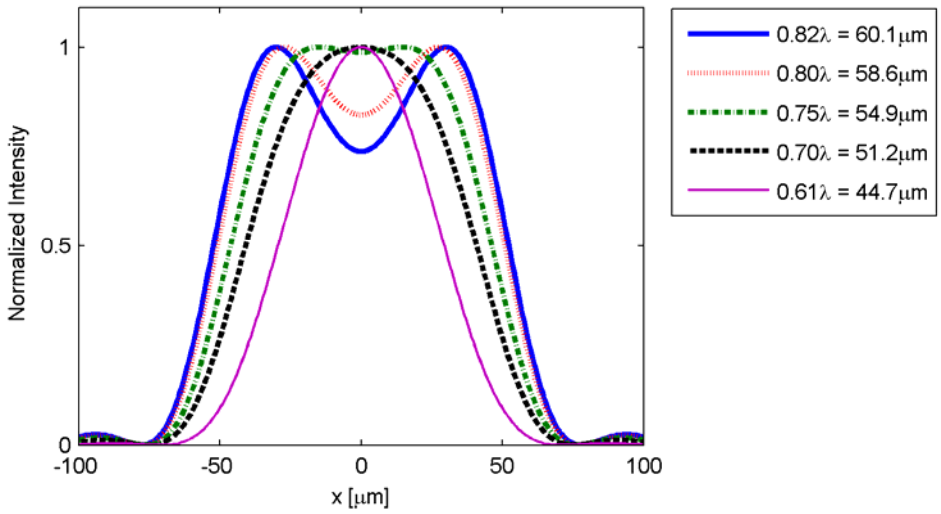

Supplementary Figure S8 | Image profiles of two 15 μm circular apertures, separated at a prescribed distance apart. The diffraction-limited imaging system has λ = 632.8 nm and NA = 0.00864. The legend shows the center-to-center aperture separations of the corresponding image profiles.